International Journal of Pressure Vessels and Piping 188 (2020) 104228

Contents lists available at ScienceDirect

International Journal of Pressure Vessels and Piping

journal homepage: http://www.elsevier.com/locate/ijpvp

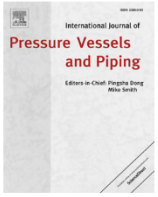

A simplified estimation procedure for the Weibull stress parameter, *m*, and applications to predict the specimen geometry dependence of cleavage fracture toughness

Vitor S. Barbosa, Claudio Ruggieri *

Department of Naval Architecture and Ocean Engineering, University of São Paulo, São Paulo, Brazil

ARTICLE INFO

Keywords:
Cleavage fracture
Local approach
Weibull stress parameter
Fracture toughness test
Specimen geometry effects

ABSTRACT

This study describes a simplified procedure to estimate the Weibull stress parameter, *m*, using cleavage fracture toughness values measured from testing high constraint fracture specimens. The estimation procedure builds upon the conventional toughness scaling methodology (TSM) based on the Weibull stress coupled with the weakest link model to correct measured toughness distributions for high constraint fracture specimens with identical in-plane dimensions but varying thickness. The approach thus requires a correspondence between predictions based upon the Weibull stress methodology and the weakest link model for measured toughness values under high constraint conditions. Applications of the proposed procedure to analyze specimen geometry effects on fracture toughness values in a typical structural steel provide predictions that agree remarkably well with experimental data for shallow crack bend specimens with different thickness. These exploratory studies demonstrate the potential capability of the proposed estimation procedure which can greatly simplify engineering integrity assessments based upon the Weibull stress model.

1. Introduction

There has been renewed interest and increased demand for developing more effective and accurate engineering analysis of the fracture behavior in critical structural components, including safety assessments and residual strength evaluation of aging structures. Much research driving these developments focuses on extensions and applications of local approaches to fracture (LAFs) to couple the (local) failure mechanism at the microlevel with the (global) macroscopic loading without explicit reference to the measure of constraint changes and its effects on macroscopic fracture toughness, as characterized by the *J*-integral and the crack tip opening displacement (CTOD) [1]. In particular, a local approach to (transgranular) cleavage fracture, introduced earlier by the Beremin group [2] and incorporating a probabilistic fracture parameter defined by the Weibull stress (σ_w), provides a tractable framework to address the complex coupling relationship between *J* (or, equivalently, CTOD) and the microscale fracture process by including implicitly the statistics of microcracks (weakest link philosophy). Recent work of Ruggieri and Dodds (R&D) [3,4] and Ruggieri et al. [5] extended the local approach concept to include the potentially strong effects of plastic strain on cleavage fracture by introducing a modified form of the Weibull stress, denoted as $\tilde{\sigma}_w$ by R&D [3]. Within this methodology, the potentially strong effects of constraint variations on fracture toughness can be described in conjunction with a relatively simple way to quantify the fracture probability. Thus, to the extent that local fracture conditions can be characterized by the Weibull stress (and, equivalently, its modified form including plastic strain effects) and, further, that cleavage fracture is driven by parameter σ_w, there is a mechanistic rationale (which is strongly connected to probabilistic arguments) for constructing a correlative procedure, often represented by a toughness scaling methodology (TSM), to analyze and unify fracture toughness measures across structural components and crack configurations of varying constraint. A full account of the local approach to cleavage fracture can be found in the review article of Pineau [6] and in recent work of R&D [3,4].

However, it became clear that the calibrated parameters defining the Weibull stress model, represented by the Weibull stress modulus, *m*, and the scale parameter, σ_u, are potentially strongly sensitive to the usual statistical variation in measured toughness values, particularly in the case of limited data sets, as well as numerical details required for accurate finite element modeling of the crack-tip stress and strain fields, including element formulation and mesh refinement. More specifically,

* Corresponding author.
E-mail address: claudio.ruggieri@usp.br (C. Ruggieri).

https://doi.org/10.1016/j.ijpvp.2020.104228
Received 20 November 2019; Received in revised form 7 September 2020; Accepted 30 September 2020
Available online 15 October 2020

one of the main difficulties with the Weibull stress approach as a broadly applicable methodology to predict effects of constraint on fracture behavior is that a relatively elaborate procedure is required to calibrate the key model parameters. Early studies addressing calibration of the Weibull parameters (see Ref. [2,7,8] for additional details), employed a single fracture toughness data set (such as J_c-values) measured from high constraint fracture specimens in connection with an iterative procedure incorporating a standard statistical method (such as the likelihood method [9]). However, Gao et al. [10] and Ruggieri et al. [11] showed later that using only a single set of fracture toughness values can lead to several pairs of parameters (m, σ_u) that satisfy equal values of the critical Weibull stress at fracture or, equivalently, equal failure probabilities for the measured fracture toughness distribution.

Those limitations also prompted Gao et al. [10] and Ruggieri et al. [11] to introduce a more effective calibration procedure based on a toughness scaling methodology using two sets of fracture toughness data measured from fracture specimens exhibiting largely different levels of constraint (triaxiality) such as, *e.g.*, deep notch and shallow notch SE(B) specimens tested at the same temperature. Their method removes the non-uniqueness of Weibull stress parameters that often arises when the calibration strategy employs only one set of fracture toughness values but at an extra cost of requiring fracture testing of different crack configurations. However, routine fracture assessments and engineering procedures to assess the significance of crack-like flaws (see API 579 [12] and BS 7910 [13] for illustrative examples) typically rely on limited testing of standard fracture specimens (such as deeply notched C(T) or SE(B) specimens), often due to severe limitations on material availability, which can make calibration of parameter m using two sets of specimens all but prohibitive. While their calibration approach represents a major advancement in previous Weibull stress models to assess constraint effects on elastic-plastic fracture toughness, simpler and yet effective schemes to calibrate the Weibull stress parameters, and more specifically the key parameter m, become necessary in routine, conventional engineering analyses.

This study describes a simplified procedure to estimate the Weibull stress parameter, m, using cleavage fracture toughness values measured from testing high constraint fracture specimens. The proposed methodology builds upon the toughness scaling model using the Weibull stress introduced earlier by R&D [8] to correct measured distributions of toughness values for fracture specimens with varying thickness. A key feature of the calibration strategy is that only one set of toughness data measured from standard specimens is needed to generate the statistical distribution for subsequent use in the calibration method. The second toughness parameter required in the toughness scaling methodology derives from application of the weakest link model to describe the effects of thickness on cleavage fracture toughness. The procedure thus requires a correspondence between predictions of thickness effects on fracture toughness generated from the Weibull stress approach and the weakest link model. This approach builds upon the same scaling procedure applied on measured toughness distributions developed by Gao et al. [10] and Ruggieri et al. [11] while, at the same time, using weakest link statistics to provide the additional toughness data needed for calibration of parameter m.

The plan of the paper is as follows. Section 2 outlines the essential features of the Weibull stress (σ_w) approach to characterize cleavage fracture in ferritic steels and the toughness scaling model based on σ_w to correct measured distributions of toughness values. Section 3 describes the proposed simplified methodology to estimate the Weibull modulus and provides the necessary framework for implementation of the estimation scheme. Section 4 summarizes the computational models and the numerical procedures employed to construct Weibull stress trajectories for fracture specimens needed to estimate parameter m, including specific details of the estimation strategy. Section 5 presents the application of the methodology to predict specimen geometry effects on cleavage fracture toughness. First, the procedure is employed to estimate the Weibull stress parameter, m, for a typical A285 Gr C pressure vessel grade steels. The analyses then consider application of the proposed approach to predict cleavage fracture behavior in low constraint fracture specimens for an A572 Gr 50 structural steel. These exploratory studies demonstrate the potential capability of the proposed estimation procedure which can greatly simplify engineering integrity assessments based upon the Weibull stress model.

2. Local approach to fracture: summary of the Weibull stress model

This section introduces the essential features of the probabilistic model for cleavage fracture based on the modified Weibull stress framework needed to unify toughness measures across different crack configurations and loading modes. The brief description that follows draws heavily on the recent work of Ruggieri and Dodds (R&D) [3,5] while, at the same time, providing the basis to introduce a simplified estimation procedure for the model parameters.

2.1. Probabilistic modeling of cleavage fracture and the Weibull stress

Experimental studies consistently reveal large scatter in the measured values of cleavage fracture toughness for ferritic steels tested in the ductile-to-brittle transition (DBT) region. A continuous probability function derived from weakest link statistics conveniently describes the distribution of toughness values, here characterized in terms of J_c-values, in the form of the standard three-parameter Weibull distribution [9] given by

$$F(J_c) = 1 - \exp\left[- \left(\frac{J_c - J_{\min}}{J_0 - J_{\min}} \right)^{\alpha} \right] \tag{1}$$

in which α defines the Weibull modulus (which characterizes the scatter in the experimental toughness data), J_0 is the characteristic toughness (which defines the J_c-value at which the failure probability is 63.2 %) and $J_{\min}$ denotes the threshold J-value for which $F(J_c) = 0$. Under conditions pertaining to well-contained yielding in the crack-tip region, the distribution of J_c-values is advantageously described by specifying a fixed value $\alpha = 2$ in the above expression, and hence Eq. (1) makes contact with a probabilistic treatment of fracture under SSY conditions based on weakest link theory [7,10,14]. Moreover, the threshold fracture toughness is often set equal to zero so that the above Weibull function assumes its more familiar two-parameter form. The above limiting distribution remains applicable for other measures of fracture toughness, such as K_{Jc} or CTOD.

Current probabilistic models to extend the above distribution to multiaxially stressed, 3-D crack configurations employ weakest link arguments to couple the micromechanical features of the fracture process (such as the inherent random nature of cleavage fracture) with the inhomogeneous character of the near-tip stress fields. Extensive experimental work on cleavage fracture in ferritic steels [15] demonstrates the key role played by Griffith-like microcracks [16] on cleavage failure - these microcracks are primarily formed by the cracking of hard, brittle particles such as carbides along grain boundaries. The statistical nature of this highly-localized fracture process prompted the development of a more refined probabilistic model to couple macroscopic fracture behavior with random microscale events. Making use of probability theory in connection with the Poisson process to describe the occurrence of Griffith-like microcracks in a reference volume, denote V_0, of the material ahead of a macroscopic crack (see, *e.g.*, Feller [17]), the elemental failure probability, δP, can be expressed as

$$\delta P = \delta V \int_{a_c}^{\infty} g(a) da \tag{2}$$

where $g(a)da$ is the probability of finding a microcrack with size between a and $a + da$ in the reference volume [18,19].

Using now weakest link arguments in connection with the maximum

principal stress criterion, Eq. (2) yields the probability distribution, P_f, for a multiaxially stressed, 3-D crack configuration in the form

$$P_f(\sigma_1) = 1 - \exp\left[-\frac{1}{V_0}\int_{\Omega}\left(\frac{\sigma_1}{\sigma_u}\right)^m dV \right] \tag{3}$$

which can be rewritten as

$$P_f(\sigma_w) = 1 - \exp\left[-\left(\frac{\sigma_w}{\sigma_u}\right)^m \right] \tag{4}$$

such that the Weibull stress, σ_w, is defined by

$$\sigma_w = \left[\frac{1}{V_0}\int_{\Omega}\sigma_1^m d\Omega\right]^{1/m} \tag{5}$$

where it is understood that the maximum principal stress, σ_1, acting on material points inside the fracture process zone enters through the dependence between the critical microcrack size, a_c, and stress in the form $a_c = K_{Ic}^2/(Y\,\sigma_1^2)$, where K_{Ic} is the (local) fracture toughness and Y represents a geometry factor associated with the microflaw. The volume of the near-tip fracture process zone, Ω, is most often defined as the loci where $\sigma_1 \geq \psi\sigma_{ys}$, in which σ_{ys} represents the material's yield stress and $\psi \approx 2$. In the above development, Eq. (4) defines a two-parameter Weibull distribution [9] in terms of σ_w with parameters m (the Weibull modulus) and σ_u (the scale parameter). Moreover, the reference volume, V_0, is conveniently assigned a unit value in routine analysis since it only scales $g(a)$ without changing the distribution shape and, thus, it has no effect on the Weibull modulus, m.

2.2. Weibull stress based toughness scaling approach

Early work of Ruggieri and Dodds [8] introduced a toughness scaling model (TSM) based upon the Weibull stress to assess the effects of constraint variations on cleavage fracture toughness data. At the heart of this methodology is the interpretation of σ_w as the (probabilistic) crack driving force coupled with the condition that cleavage fracture occurs when σ_w reaches a critical value, $\sigma_{w,c}$. For the same material at a fixed temperature, the scaling model postulates that cleavage fracture across crack configurations with varying levels of constraint occurs at a fixed, critical value of σ_w. Within the present probabilistic context, attainment of a critical value of the Weibull stress in different cracked configurations translates into equal probability for cleavage fracture.

Fig. 1(a) illustrates the procedure to assess the effects of constraint loss on cleavage fracture behavior needed to scale toughness values for different cracked configurations. The method begins by performing very detailed, nonlinear 3-D finite element analyses to determine the functional relationship between σ_w and applied loading for a specified value of the Weibull modulus, m. By using J to characterize macroscopic loading (the approach remains equally applicable for other measures of macroscopic loading, such as K_{Jc} or CTOD), construction of Weibull stress trajectories for a high constrained configuration (such as a deep notch SE(B) specimen), represented by configuration **A**, and a low constraint configuration (such as single notch tension SE(T) specimen), represented by configuration **B**, enables establishing the toughness correction $J_{0,A} \rightarrow J_{0,B}$ as indicated in the figure.

3. A simplified estimation procedure for the Weibull stress parameters

3.1. Perspectives on current calibration methods

Parameter calibration of the Weibull modulus, m, represents a key step in predictive applications of the LAF methodology based on the Weibull stress concept previously outlined. The scale parameter, σ_u, follows directly from the σ_w-value corresponding to $P_f = 63.2$ % in Eq. (4) once m is determined. Current procedures to estimate the Weibull stress parameters (see Ref. [10,11] for additional details), employ the toughness scaling model introduced in Section 2.2 to determine parameter m based upon the Weibull stress trajectories generated from two crack configurations exhibiting different constraint levels (*e.g.*, a deep notch and a shallow notch SE(B) specimen). The approach seeks the parameter m which best corrects the probability distribution of J_c-values of one configuration to the corresponding J_c-distribution of another configuration (see R&D [3,4] for details), thereby removing the non-uniqueness of the calibration procedure associated with the use of only one fracture toughness data set [10,11]. Within this methodology, calibration of the Weibull stress parameters can thus be associated with an inverse problem strategy in which a given set of representative data is used to adjust the model response until the calibrated parameters enable the model to best fit the experimental measurements.

However, despite its effectiveness in applications to predict cleavage fracture behavior in typical structural steels, including pressure vessel grade steels, in the DBT region (see, *e.g.*, the representative works of Gao et al. [20], Gao and Dodds [21,22], Petti and Dodds [23,24], Ruggieri [25,26] and R&D [3,5]), a practical objection to the Gao et al. approach [10] is that it requires fracture testing of different crack configurations and/or specimen geometries. As already mentioned, routine fracture analysis and defect assessment procedures are typically based on limited testing of conventional fracture specimens which can make calibrations

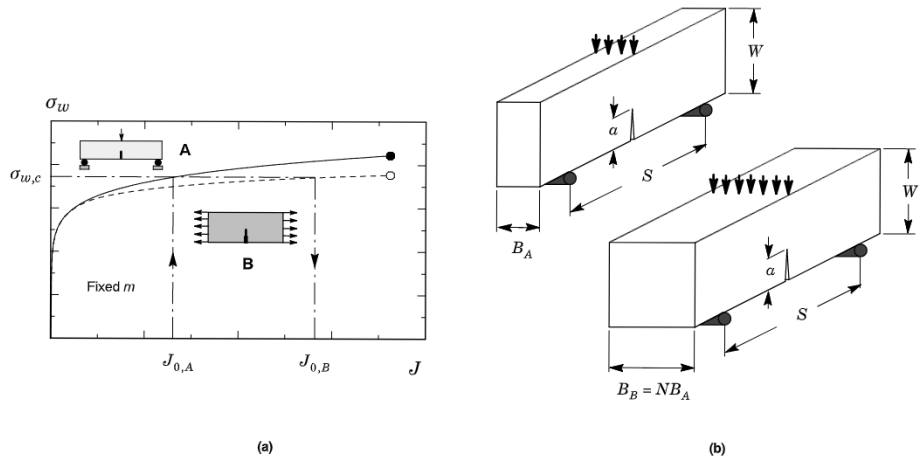

Fig. 1. (a) Toughness scaling model (TSM) based on the Weibull stress concept to correct fracture toughness due to constraint and specimen geometry effects. (b) Schematic of two fracture specimens with identical in-plane dimensions but different thickness to illustrate application of the weakest link model.

of the Weibull stress parameters using two sets of specimens a rather complex task. Moreover, the calibrated parameters, including more specifically the Weibull modulus, are usually somewhat sensitive to the specimen configurations used in this two-set approach and, thus, are not necessarily applicable in a predictive manner over a broad range of loading and geometry configurations. The large differences in reported values of parameter m for common pressure vessel and structural steels (several previous studies found m-values in the range between 10 and 40~50) reveal an uncertain picture of current calibration methods with potential serious implications for the Weibull stress based fracture methodology.

Other recent efforts in this area include the related works by Andrieu et al. [27], Cao et al. [28] and Qian et al. [29]. To some extent, all these approaches share a similar basis in which only a single set of fracture toughness values derived from high constraint specimens is employed to perform the parameter calibration but they differ in the strategy to estimate parameter m. In particular, Cao et al. [28] and Qian et al. [29] adopt a calibration method similar to the procedure previously proposed by Minami et al. [7] but with the incorporation of a Monte Carlo simulation to generate a large number of fracture toughness values from which an iteration procedure now yields the estimated m-value. However, since the generated large data set of fracture toughness values does not remove the uncertainties arising from the calibration procedure proposed in Ref. [7] (see the detailed discussion provided by Gao et al. [10] and Ruggieri et al. [11]), it is not clear whether their approach has the capability to avoid the nonuniqueness of the calibrated parameters which, in turn, can lead to large uncertainties in parameter m.

The calibration methodology developed by Andrieu et al. [27] also deserves further discussion. Making use of the asymptotic HRR stress solution [30–32] strictly valid for a plane-strain idealization of a fracture specimen having thickness B, they approached the calibration problem by first expressing the Weibull stress, σ_w, in a separable form as $\sigma_w^m = BK_J^4\sigma_0^{m-4}C_{m,n} / V_0$, where $C_{m,n}$ is a function of material flow properties and m, but independent of loading, and then assuming the product $K_J^4\sigma_0^{m-4}$as a constant value for a fixed failure probability. We note that Andrieu et al. [27] expressed σ_w in terms of K_I whereas here we use the elastic-plastic parameter K_J. Their procedure relies on a best fitting procedure to the measured variation of K_J with σ_0 to yield an estimate of parameter m. While this methodology has a sound underlying micromechanics basis, a major drawback in engineering applications of their approach is that it still requires fracture toughness testing at different temperatures to obtain measured K_J-values with varying temperature-dependent flow properties in the ductile-to-brittle transition region.

3.2. New proposal to estimate the Weibull stress parameter, m

The continuous probability function derived from weakest link statistics to characterize the distribution of toughness values expressed by previous Eq. (1) provides the starting point for the introduction of the new calibration procedure. Because the Weibull distribution defined by the above Eq. (1) is directly connected to a type III extreme value distribution [9,33,34], it allows direct application to a weakest link scaling model to describe the observed effects of specimen thickness on fracture toughness. Consider two high constraint specimen configurations, denoted as **A** and **B**, with identical in-plane dimensions but different thickness as pictured in Fig. 1(b). Assuming that configuration **B** consists of $N = B_B/B_A$ times specimen **A** and invoking the weakest link model with $J_{min} = 0$ for convenience in Eq. (1), parameter $J_{0,A}$ is simply scaled to the characteristic toughness for configuration **B** (which has different thickness), $J_{0,B}$, by

$$J_{0,B} = (B_A/B_B)^{(1/\alpha)}J_{0,A} \tag{6}$$

in which B_A and B_B represent the specimen thickness for configurations **A** and **B** as shown in Fig. 1(b).

The above expression is adopted by several other works and studies, including the Master Curve standard described by ASTM E1921 [35], and derives directly from the weakest link scaling property associated with the dependence of the fracture stress for a stressed solid on the statistical population of microflaws uniformly distributed over its volume V (see the review article by Ruggieri and Dodds [3]). A requisite assumption for strict application of Eq. (6) is that the fracture toughness distributions of configurations **A** and **B** have the same scatter, that is, the same Weibull modulus, α (refer to Eq. (1) in previous section). Further, Eq. (6) remains valid only to scale cleavage fracture toughness distributions for effects of thickness not for effects of crack tip constraint. Consequently, in applying the above procedure to estimate the characteristic toughness, $J_{0,B}$, configurations **A** and **B** must have the same a/W-ratio but with different thickness. As will be presented later, it is most convenient to take configuration **A** as a standard 1T, high constraint fracture specimen having $a/W = 0.5$~0.6 to obtain the experimentally measured fracture toughness distribution from which the reference characteristic fracture toughness, $J_{0,A}$, can be determined.

The thickness correction expressed by Eq. (6) thus provides the second toughness parameter required in applications of the TSM illustrated in Fig. 1(a). Consequently, the calibrated m-value for the material is defined as the value at which $J_{0,A}\rightarrow J_{0,B}$. This condition enforces a correspondence between predictions based on the Weibull stress approach and the weakest link model for measured toughness values for a high constraint specimen. The approach builds upon the same scaling procedure to correct measured toughness distributions developed by Gao et al. [10] and Ruggieri et al. [11] while, at the same time, using the weakest link model to provide the additional toughness data needed for calibration of parameter m. While there exist no strict requirements for a specific choice of the thickness ratio as the basis for the scaling $J_{0,A}\rightarrow J_{0,B}$, the two crack configurations (**A** and **B**) must have sufficiently different σ_w vs. J histories computed for the same m-values to insure appropriate levels of $J_{0,A}/J_{0,B}$-ratios. Moreover, for a given $J_{0,A}/J_{0,B}$-ratio (which corresponds to two crack configurations with thickness B_A and B_B), the estimated m-parameter is expected to depend on the flow properties for the tested material.

At this point, we also want to further discuss the applicability of the proposed approach for the particular case of a plane-strain idealization of a fracture specimen having thickness B and under restricted levels of deformation such that the near-tip fields follow well-contained, small scale yielding (SSY) conditions. Here, the characteristic structure of these fields assume a self-similar form in which the J-integral sets the scale of deformation at the crack tip analogous to the HRR solution [32,36]. Under such conditions, Gao et al. [10] showed that the characteristic toughness, J_0, is related to the Weibull stress parameters by

$$J_0^2 = \frac{V_0\sigma_u^m}{B\Phi\sigma_{ys}^{m-2}} \tag{7}$$

where Φ is a function of material flow properties and m, but independent of J. While the functional form shown in Eq. (7) applies only for strict 2-D plane-strain SSY conditions, it reveals an important feature associated with the non-uniqueness of the Weibull stress parameters since, for a know J_0-value from test data, many (m, σ_u) pairs can be obtained to satisfy Eq. (7). Consequently, it becomes apparent that, in the limit case of 2-D plane-strain SSY conditions, no unique solution can exist and, hence, the proposed approach may be insufficient robust to provide a viable basis for fracture mechanics applications.

However, standard fracture specimens with finite size and thickness exhibit crack front conditions with a 3-D character that deviate rather significantly from these theoretical conditions, particularly for material points over the crack front that approach the stress-free surface of the specimen. In this regard, the numerical studies of Nevalainen and Dodds [37] and Ruggieri et al. [5,38] provide examples of the strong variation of the stress fields across the crack front for standard fracture specimens. Thus, while we make no claim that the present procedure leads to a

unique pair of (m, σ_u) parameters, the proposed method in connection with Eq. (6) should provide a convenient and simple route to estimate the Weibull stress parameters with relatively modest effort. Section 6 addresses this issue in more details and illustrates applications of the procedure to calibrate the Weibull stress modulus and to predict cleavage fracture in a ferritic structural steel.

4. Fracture toughness testing

4.1. ASTM A285 Gr C steel

Savioli and Ruggieri [39] (see also Ruggieri [38]) conducted fracture mechanics tests on conventional plane-sided 1T SE(B) specimens with $a/W = 0.5$, $B = 25$ mm, $W = 50$ mm and $S = 4W$. The material is a typical ASTM A285 Grade C pressure vessel steel with 230 MPa yield stress and 450 MPa tensile strength at room temperature (20°C). Uniaxial tensile tests performed on cylindrical specimens with 12.5 mm diameter extracted from the transversal plate direction at mid-thickness location provide the room temperature mechanical data. Moreover, additional tensile tests were also conducted on subsize test specimens with 6 mm diameter at $T = -80$°C . Table 1 summarizes the tensile testing results for this material where it is evident the high hardening behavior of the tested steel with $\sigma_{uts}/\sigma_{ys} \approx 2$ at room temperature. Other mechanical properties for this material include Young's modulus, $E = 204$ GPa and Poisson's ratio, $\nu = 0.3$.

Fig. 2(a) shows the experimentally measured J_c-values for the tested specimens under discussion. To make contact with the two-parameter Weibull function describing the cleavage fracture stress defined by previous Eq. (3) later in the calibration procedure, the cumulative distribution of the experimental data is represented by the Weibull distribution for J_c-values expressed by Eq. (1) with $J_{min} = 0$. In this plot, the solid symbols represent cleavage toughness values, whereas the probability function $F(J_c)$ is given by adopting a conventional median ranking of the ordered fracture data in which $F(J_{c,k}) = (k - 0.3)/(N + 0.4)$, where k is the fracture toughness order number and N is the total number of fracture data [9]. The standard deformation limit values, described by $M = (W - a)\sigma_{ys}/J$, for the tested deeply-cracked SE(B) specimens with $a/W = 0.5$ reported by Ruggieri [38] show that the measuring toughness capacity for this configuration is well above the M-values corresponding to small scale yielding thereby clearly indicating well-defined cleavage fracture under essentially stress-controlled conditions. Following a standard maximum likelihood (ML) procedure [9] with $\alpha = 2$ and $J_{min} = 0$, the estimate of the characteristic toughness for the distribution of J_c-values shown in Fig. 2(a) yields $J_0 = 73$ kJ/m^2.

4.2. ASTM A572 Gr 50 steel

Barbosa and Ruggieri (B&R) [40] carried out a series of fracture tests on three-point bend fracture specimens with varying geometry in the T-L orientation. The tested geometries used in the present analysis include conventional, plane-sided 1T SE(B) specimens with $a/W = 0.5$ and $a/W = 0.2$, $B = 25$ mm, $W = 50$ mm and $S = 4W$. Here, a is the crack size, W denotes the specimen width, B represents the specimen thickness and S is the load span. Fracture tests were also conducted on conventional,

Table 1
Tensile properties of tested steels at different test temperatures measured from transverse plate direction at mid-thickness location (σ_{ys} and σ_{uts} denote the yield stress and tensile strength while n is the strain hardening exponent.

Material	T (°C)	σ_{ys} (MPa)	σ_{uts} (MPa)	σ_{uts}/σ_{ys}	n
A285 Gr C	20	230	446	1.9	5.3
	−80	342	512	1.5	7.9
A572 Gr 50	20	376	555	1.5	8.0
	−20	407	601	1.5	8.0

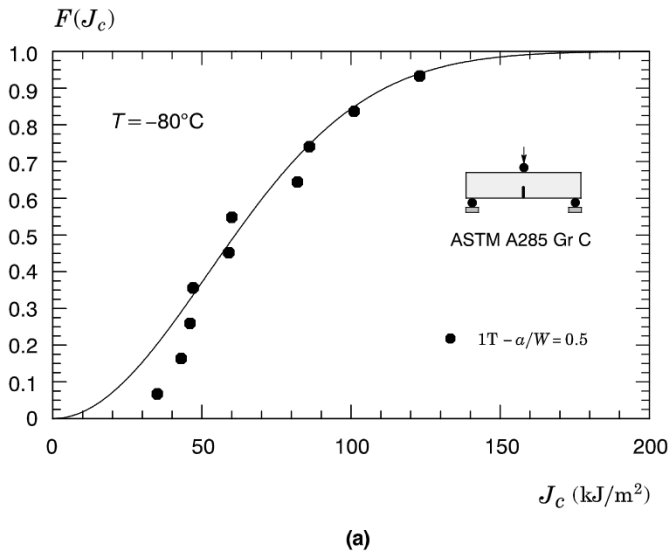

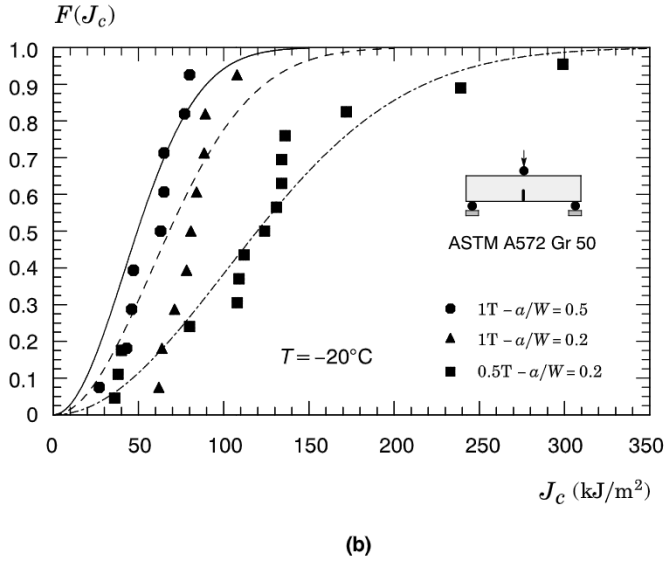

Fig. 2. Cumulative Weibull distribution of experimentally measured J_c-values for the tested materials: (a) A285 Gr C pressure vessel steel at $T = -80$°C. (b) A572 Gr 50 structural steel at $T = -20$°C.

plane-sided SE(B) specimens with $a/W = 0.2$ and $W = 50$ mm ($S = 4W$) but with a reduced thickness of 0.5T with $B = 12.5$ mm. The material is a typical ASTM A572 Grade 50 structural steel with 376 MPa yield stress and 555 MPa tensile strength at room temperature (20°C). Testing of these configurations was performed at $T = -20$°C which corresponds to near lower-shelf behavior for the material (see CVN data in B&R [40]). Mechanical tensile tests conducted on standard tensile specimens with 12.5 mm diameter extracted from the transverse plate direction at mid-thickness location provide the room temperature stress-strain data. Since the fracture tests were conducted in the DBT region of the material, additional tensile tests were also conducted at $T = -20$°C on subsize test specimens with 6 mm diameter. Other mechanical properties for this material include Young's modulus, $E = 201$ GPa and Poisson's ratio, $\nu = 0.3$. Fig. 3(a) provides the engineering stress-strain curve for the ASTM A572 Grade 50 steel at room temperature and at $T = -20$°C (average stress-strain response using data from three standard test specimens). Table 1 provides the tensile testing results for this material at different temperatures. Fig. 3(b) shows the conventional Charpy V-notch impact energy with for the material in the T-L orientation. Table A.1 in the Appendix shows the J_c-values obtained at $T = -20$°C

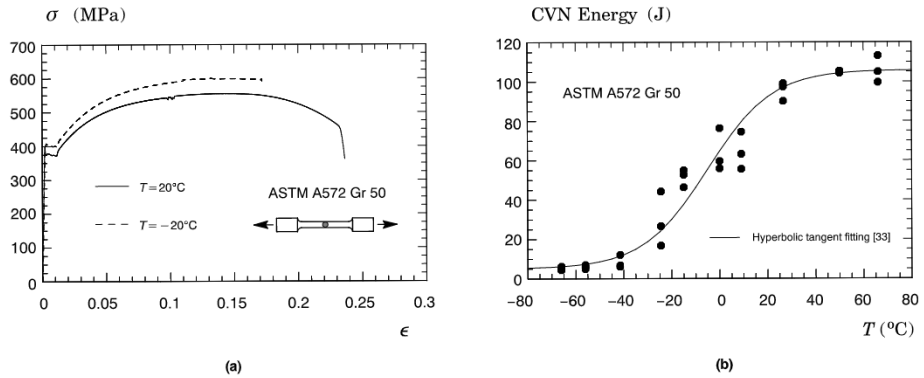

Fig. 3. (a) Engineering stress-strain curve (average stress-strain response using data from three test specimens) for the tested A572 Gr 50 steel at different temperatures. (b) Charpy-V impact energy (T-L orientation) versus temperature for the tested A572 Gr 50 steel.

Table 2
Maximum likelihood estimates of parameter J_0 for the measured distributions of J_c-values of each tested specimen geometry, including the predicted values for the A572 steel.

Geometry	B (mm)	α	$J_{0\text{-}MLH}$ (kJ/m^2)	$J_{0\text{-}WLM}$ (kJ/m^2)	$J_{0\text{-}MC}$ (kJ/m^2)
SE(B) - $a/W = 0.5$	25	2	59	n.a.	n.a.
SE(B) - $a/W = 0.2$	25	2	82	84	n.a
SE(B) - $a/W = 0.2$	12.5	2	141	144	155

from the shallow crack bend specimens with $a/W = 0.2$ and reduced thickness of $B = 12.5$ mm - these toughness values are not reported in the work of B&R [40] and are presented in this study for completeness.

Fig. 2(b) shows Weibull distribution of the measured J_c-values, here represented by the solid symbols, for the tested deeply-cracked SE(B) specimens given by Eq. (1) with $J_{min} = 0$. In the plot, the probability function $F(J_c)$ is given by adopting the same median ranking of the ordered fracture data already described for the A285 steel. Table 2 provides the ML estimates of the characteristic toughness, J_0, for all tested crack configurations, including the shallow crack specimens with $B = 12.5$ mm. Moreover, similarly to the previous results, the M-values reported by B&R [40] show that the measured J_c-values for the deeply-cracked specimen also describe cleavage fracture under essentially stress-controlled conditions.

5. Finite element procedures

5.1. Finite element models

Numerical analyses are performed on 3-D models of the fracture specimens previously described to generate the crack-tip stresses to compute the evolution of σ_w versus J needed in the parameter estimation procedure and predictions of fracture toughness described next. Fig. 4(a) shows the quarter-symmetric, 3-D models of the tested deeply cracked 1T SE(B) specimen with $a/W = 0.5$. The numerical models for other specimen configurations have very similar features with the same in-plane mesh but varying thickness covering $B = 12$ mm (0.5T), $B = 50$ mm (2T), $B = 75$ mm (3T) and $B = 100$ mm (4T). A conventional mesh configuration having a focused ring of elements surrounding the crack front as pictured in Fig. 4(b) is used with a small key-hole at the crack tip; the radius of the key-hole, ρ_0, is 2.5 μm (0.0025 mm). Symmetry conditions enable analyses using one-quarter of the 3-D models with appropriate constraints imposed on the symmetry planes. The quarter-symmetric, finite element model for the SE(B) geometry displayed in Fig. 4(a) consists of 34 variable

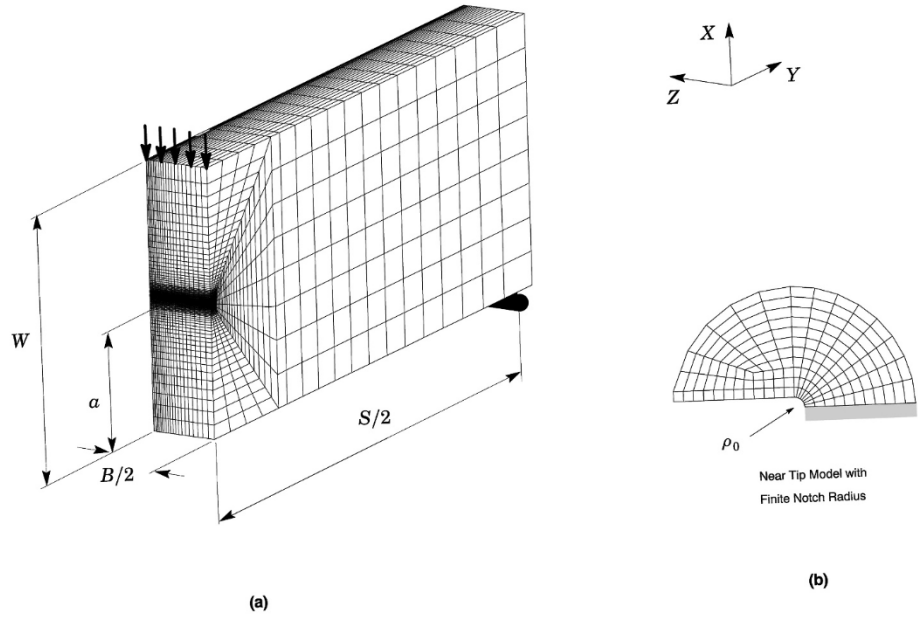

Fig. 4. (a) Finite element model used in the 3-D analyses of the plane-sided SE(B) fracture specimens with $a/W = 0.5$ and 1T geometry. (b) Near-tip finite element model with a blunt notch radius of $\rho_0 = 0.0025$ mm.

thickness layers (approximately 41000 nodes, 46000 3-D elements).

The blunting notch radius represents an implicit length-scale entering the numerical analysis as the Weibull stress is computed by raising the near-tip principal stress to a large power characterized by parameter m - refer to Section 2. Previous studies conducted by Ruggieri and Dodds [4] show a relatively weak influence of ρ_0 on σ_w-values and, consequently, on fracture predictions within the range $0.0025\ \text{mm} \leq \rho_0 \leq 0.01\ \text{mm}$. Section 6.2 further addresses this issue for the fracture specimens and parameter estimation under consideration.

5.2. Material model and solution procedures

The finite element computations to generate the required evolution of σ_w vs. J described next follow nonlinear procedures incorporated in WARP3D [41] which: 1) implements a Mises plasticity models in a finite-strain framework; 2) evaluates the J-integral using a convenient domain integral procedure [42] and 3) utilizes fracture models constructed with three-dimensional, 8-node hexahedral elements. The code formulates and solves the equilibrium equations at each iteration using parallel algorithms and implements the so-called $\overline{\mathbf{B}}$ formulation (see Refs. [41] for details) to avoid mesh lock-ups that may occur during fully plastic, incompressible modes.

For the tested A285 pressure vessel steel, a simple power-hardening model to characterize the uniaxial true stress *vs.* logarithmic strain in the form

$$\frac{\overline{\varepsilon}}{\varepsilon_{ys}} = \frac{\overline{\sigma}}{\sigma_{ys}} \quad , \quad \overline{\varepsilon} \leq \varepsilon_{ys} \quad ; \quad \frac{\overline{\varepsilon}}{\varepsilon_{ys}} = \left(\frac{\overline{\sigma}}{\sigma_{ys}}\right)^{n} \quad , \quad \varepsilon > \varepsilon_{ys} \tag{8}$$

is employed, in which σ_{ys} and ε_{ys} are the (reference) yield stress and strain, and n denotes the strain hardening exponent. Here, we use Annex F of API 579 [12] to obtain an improved estimate of the strain hardening exponents at the test temperature (refer to Table 1) as $n = 7.9$ at $T = -80$°C. For the tested A572 steel, a piecewise linear approximation to the measured tensile response for the material is employed with the true stress-logarithmic strain curves at $T = -20$°C obtained from the engineering tensile response shown in Fig. 3(a).

Numerical computations of the Weibull stress used to construct $\sigma_w$vs. J trajectories are performed using the research code WSTRESS [43] which implements a finite element form of previous Eq. (5). In isoparametric space, the current (deformed) Cartesian coordinates of any point inside a 8-node tri-linear element are related to the parametric coordinates using the shape functions corresponding to the k-th node. Let $\mathbf{D}$ denote the determinant of the standard coordinate Jacobian between deformed Cartesian and parametric coordinates. Then using standard procedures for integration over element volumes, the Weibull stress has the form

$$\sigma_w = \left[\frac{1}{V_0}\int_{\Omega} \sigma_1^m d\Omega\right]^{1/m} = \left[\frac{1}{V_0}\sum_{n_e}\int_{-1}^{1}\int_{-1}^{1}\int_{-1}^{1} \sigma_1^m \mathbf{D} d\eta_1 d\eta_2 d\eta_3\right]^{1/m} \tag{9}$$

where n_e is the number of elements inside the fracture process zone near the crack tip. As already mentioned, the fracture process zone used includes all material inside the loci, $\sigma_1 \geq \psi\sigma_{ys}$, with $\psi \approx 2$. However, since the Weibull stress is evaluated by raising the σ_1 to a large power characterized by parameter m, it becomes clear that σ_w and, consequently, the estimated Weibull stress parameters and fracture predictions differ little over a relatively wide range of ψ-values. For computational simplicity, an element is included in the fracture process zone if the computed σ_1 at $\eta_1 = \eta_2 = \eta_3 = 0$ (*i.e.*, the geometric center of the element) exceeds $\psi\sigma_{ys}$.

6. Applications to fracture toughness testing

6.1. Calibration of the Weibull modulus using the simplified procedure

The proposed simplified procedure previously presented is employed here to estimate the Weibull modulus, m, for the two structural steels described in Section 4. The process begins by scaling the characteristic toughness, J_0, of the Weibull distribution describing the

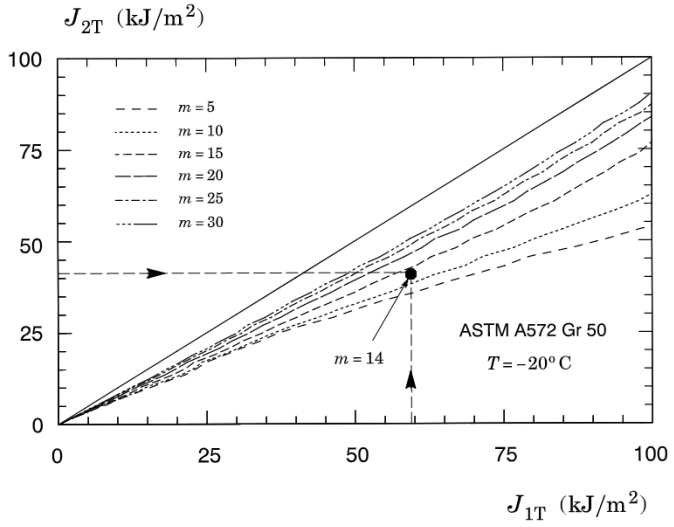

Fig. 6. Toughness scaling for the SE(B) specimens with 1T ($B = 25$ mm) and 2T ($B = 50$ mm), denoted $J_{1T} \rightarrow J_{2T}$ scaling, with varying Weibull moduli, m, for the ASTM A572 steel.

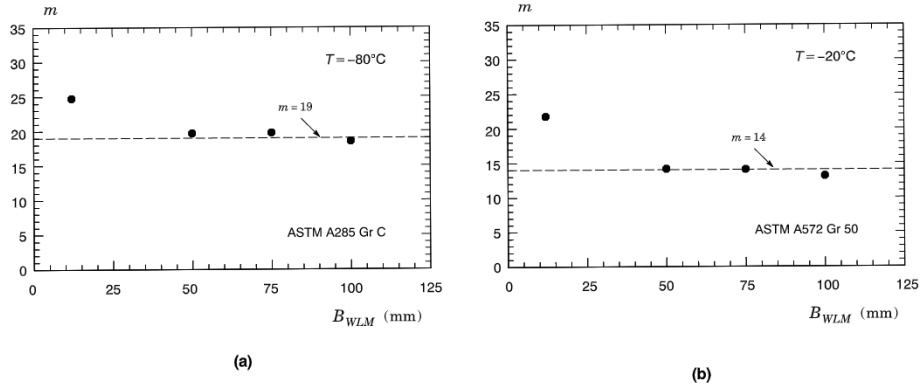

Fig. 5. Effect of varying specimen thickness considered in the estimation procedure for configuration **B**, B_{WLM},on the estimated Weibull modulus, m: a) A285 pressure vessel steel. (b) A572 structural steel.

measured J_c-values obtained from testing the 1T SE(B) specimen with $a/W = 0.5$ for each material (taken here as configuration **A** with $J_0^A = 73$ kJ/m^2 for the A285 steel and $J_0^A = 59$ kJ/m^2 for the A572 steel) to the corresponding J_0-value of an SE(B) geometry with $a/W = 0.5$ with different thickness (taken as configuration **B**) such that a thickness correction derived from the weakest link model holds true - observe that this procedure is essentially equivalent to scaling the probability distribution of J_c-values of one configuration to the corresponding J_c-distribution of another configuration (see R&D [3,4] for details). Here, the estimated Weibull modulus satisfies a minimization procedure for the residual function defined by $R(m) = (J_{0,m}^A - J_0^A)/J_0^A$ with $R(m) \approx 0.01$. The research code WSTRESS [43] is employed to generate the required σ_w vs. J trajectories and to estimate parameter m for the cases under consideration.

Consider first estimation of parameter m for the ASTM A285 steel. The effect of varying the specimen thickness considered in the estimation procedure for configuration **B**, here denoted B_{WLM}, is displayed in Fig. 5(a). Observe that an almost constant m-value of ≈ 19 is practically attained when B_{WLM} is larger than 50 mm, which corresponds to a 2T specimen configuration. In contrast, it is of interest to note that parameter m increases rather sharply with decreased specimen thickness ($B = 12$ mm) relative to the reference thickness of 25 mm. Indeed, this behavior could be anticipated as fracture specimens with reduced thickness increasingly violate the weakest link model upon which the proposed estimation procedure is based. The results given in that plot thus show that the estimated Weibull modulus for the material under consideration can be taken as $m = 19$. Such estimated value is close to the calibrated value of 17 reported by Ruggieri [38] for this material obtained from using the Weibull stress trajectories for two crack configurations represented by a deep notch and a shallow notch SE(B) specimen. Consider next the effect of specimen thickness, B_{WLM}, used in the estimation procedure of parameter m for the ASTM A572 steel shown in Fig. 5(b). The overall trends remain similar except that now a constant m-value of ≈ 14 is attained when B_{WLM} is larger than 50 mm. Thus, within the proposed procedure, the value of $m = 14$ is taken as the estimated Weibull modulus for the tested A572 steel.

The potential influence of varying Weibull moduli on the estimation of parameter m is also of interest. Fig. 6 provides the scaling of toughness for the 1T and 2T SE(B) geometries ($J_{1T} \rightarrow J_{2T}$ scaling) with varying Weibull moduli, m, for the ASTM A572 steel. The present computations consider values of m in the range $5 \leq m \leq 30$ to assess the sensitivity of the toughness scaling on parameter m. These m-values are consistent with previously reported values for structural steels [2,7,8,10,11,20,25,44]. Each curve provides pairs of J-values, for the 1T SE(B) and the 2T SE(B) specimens, that produce the same σ_w-value (refer to previous Section 2.2). A reference line is shown which defines a unit ratio of applied J-values in the 1T and 2T SE(B) specimens, *i.e.*, $J_{1T} = J_{2T}$. The significant features include: (1) For each value of parameter m, the toughness correction curves agree very well early in the loading history while both specimens maintain essentially similar near-tip stress fields along the crack front; (2) with increased loading, the near-tip stress fields remain similar on the mid-thickness plane, but vary at positions on the crack front along the thickness for both specimens thereby changing the scaling curves with varying m-values and (3) for a fixed load level in the reference geometry (1T specimen), the ratio that generates equivalent Weibull stresses at fracture increases with decreased values of the Weibull modulus as smaller m-values assign a larger weight factor to the highly stressed material volume along the crack front. More importantly, though, the trends displayed in the plot of Fig. 6 show clearly that the ratio J_{2T}/J_{1T} is sensitive to the choice of parameter m thereby providing further support to the proposed estimation procedure. Indeed, the lines shown in the plot show that the correct scaling of J_0-values for the case under consideration is satisfied for $m = 14$.

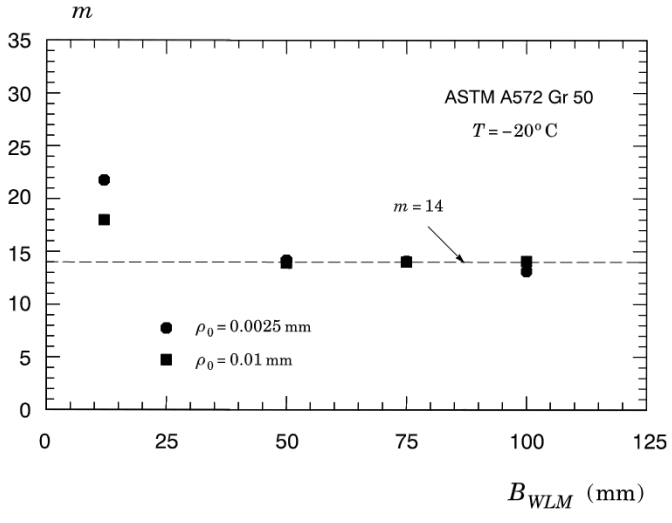

Fig. 7. Effect of different blunt notch sizes, $\rho_0 = 0.0025$ mm and $\rho_0 = 0.01$ mm, on the estimated Weibull modulus, m, for the ASTM A572 steel.

6.2. Mesh dependency analysis

Fracture analyses using the Weibull stress approach may exhibit potential problems related to finite element modeling details, including specifically mesh refinement in the crack tip region. Because σ_w derives from the principal stress raised to a large power defined by parameter m (see Eq. (5)), insufficient mesh refinement may affect peak stress values over distances of order a few CTODs thereby impacting the computed Weibull stress values and, thus, the predictive response of the Weibull stress approach. While typical finite element meshes for standard fracture analyses employ small notch root radii (blunt notch sizes defined by $\rho_0 = 0.0025$ mm are commonly used - see Gao et al. [10] for illustrative example), larger initial root radii must often be used to generate converged numerical solutions over the entire loading history for the fracture specimens under consideration.

To address this issue, Fig. 7 shows the effect of varying thickness, B_{WLM}, entering the estimation procedure of parameter m for the ASTM A572 steel considering two different blunt notch sizes, $\rho_0 = 0.0025$ mm and $\rho_0 = 0.01$ mm. The trend is clear. As could be expected, the estimated Weibull modulus display some sensitivity to the blunt notch size but which has nevertheless essentially no significant effect on the estimation of parameter m when B_{WLM} is larger than 50 mm. The results for the specimen with reduced thickness ($B = 12$ mm) relative to the reference geometry exhibit larger dependence on the blunt notch size, which seems consistent with the behavior displayed by this configuration already noted in previous section. Overall, however, since the fracture toughness scaling, $J_{1T} \rightarrow J_{B_{WLM}}$, adopted in proposed estimation procedure relies on the σ_w-trajectories for *both* specimen geometries, small relative changes in *both* σ_w-curves have only a small effect on the toughness scaling provided the conditions underlying the weakest link model are well satisfied.

6.3. Predictions of specimen geometry effects on fracture toughness

To verify the capability of the proposed estimation procedure in engineering assessments of cleavage fracture behavior, the Weibull modulus previously determined for the ASTM A572 Gr 50 steel is employed to predict the cleavage fracture distribution for the shallow crack SE(B) specimens with varying specimen thickness using the J_c-distribution for the bend geometry with $a/W = 0.5$. The procedure used here follows the toughness scaling model (TSM) laid out in Section 2.2 by postulating a critical value of the Weibull stress at fracture, $\sigma_{w,c}$, to scale the J_0-value describing the toughness distribution for the deeply-cracked SE(B) specimen to the corresponding J_0-values of the

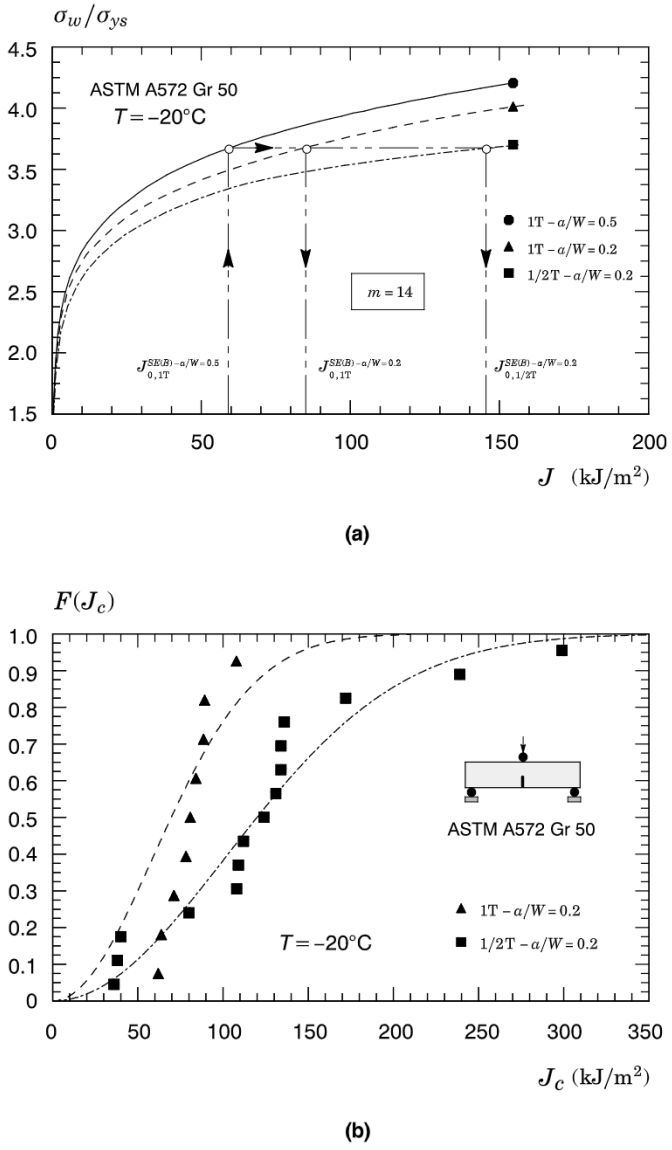

Fig. 8. (a) σ_w vs. J trajectories for the deep crack and shallow crack SE(B) specimens at $T = -20°C$ with $m = 14$. (b) Predicted cumulative two-parameter Weibull distribution of experimentally measured J_c-values for the shallow crack SE(B) specimens using the toughness distribution for the deeply-cracked bend geometry.

toughness distributions for the shallow crack bend specimens with $B = 25$ mm and $B = 12.5$ mm. Once the J_0-value for each specimen configuration is determined, the corresponding predicted distribution of fracture toughness is obtained by generating a Weibull distribution given by Eq. (1) with $\alpha = 2$ and $J_{min} = 0$.

Fig. 8(a) displays the variation of σ_w normalized by the material yield stress, σ_{ys}, with J with $m = 14$ for all specimen geometries considered here and clearly indicate the scaling procedure to determine the J_0-values for the shallow crack bend specimens with $B = 25$ mm and $B = 12.5$ mm. Using the Weibull stress at fracture determined from $J_0 = 59$ kJ/m^2 for the deeply-cracked 1T SE(B) specimen, the scaling procedure then yields $J_0 = 84$ kJ/m^2 for the shallow crack 1T SE(B) specimen and $J_0 = 144$ kJ/m^2 for the shallow crack bend specimen with $B = 12.5$ mm as shown in Table 2. The agreement of the predicted values with the J_0-values of the corresponding Weibull distributions is remarkably close. The predicted fracture toughness distributions for the shallow crack bend specimens are shown in Fig. 8(b). In these plots, the solid lines represent the predicted median values of fracture probability whereas the measured J_c-values, are represented by the solid symbols. As could be anticipated from the previous findings, the predicted distribution is in good accord with the experimental data and, further, it compares very well with the fitted Weibull distribution provided in Fig. 2.

6.4. Further simplification - exploratory toughness prediction using the Master Curve approach

The simplified estimation procedure for determining parameter m discussed thus far still relies on obtaining an experimental distribution of cleavage fracture toughness values measured from testing a high constraint fracture specimen, such as a deeply-cracked 1T SE(B) or 1T C(T) specimen, thereby providing the reference toughness distribution entering the estimation method. An alternative and simpler approach involves the use of approximate relationships between fracture toughness and Charpy V-notch impact (CVN) energy in connection with the Master Curve methodology [35,45]. In related study, Smith et al. [46] made attempts to predict fracture toughness measured from testing three-point SE(B) specimens directly from experimentally measured CVN impact energy using a Weibull stress scaling model. While their work has provided a viable basis for relating Charpy energy to fracture toughness in the lower transition region, it still relies on a rather elaborated estimation procedure for the Weibull modulus, m, based on the relationship between absorbed energy and σ_w. The approach presented here differs from that analysis in an important way since it seeks to estimate a baseline, representative fracture toughness for the material under consideration directly from the CVN energy.

The process begins by estimating the Master Curve reference temperature, T_0, directly from the CVN energy, using the expression given in ASTM E1921 [35] as

$$T_0 = T_{28J} - 18°C \quad (\pm 15°C)\,, \tag{10}$$

where T_0 is the reference (indexing) temperature at which the median toughness of a measured toughness distribution in terms of K_{Jc}-values for a 1T size, high constraint fracture specimen, denoted $K_{Jc,med-1T}$, is 100 MPa$\sqrt{\text{m}}$, and T_{28J} defines the Charpy transition temperature corresponding to 28 J.

Once T_0 is determined from Eq. (10), an estimate of J_0 for the 1T size, high constraint fracture specimen tested at temperature T is given by

$$J_0 = 1201\,\frac{\{30 + 70\exp[0.019(T - T_0)]\}^2}{E'} \tag{11}$$

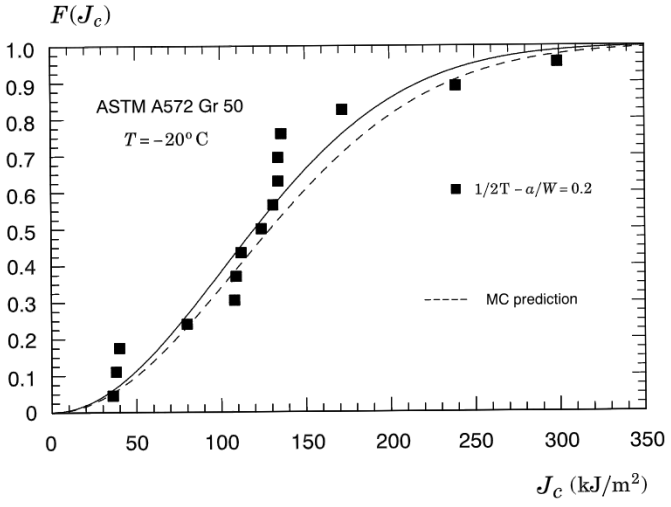

Fig. 9. Predicted cumulative two-parameter Weibull distribution of experimentally measured J_c-values for the shallow crack SE(B) specimens using the Master Curve approach.

where $E' = E/(1-\nu^2)$ and the standard relationship $J_0 = K_0^2/E'$ were assumed [36]. To arrive at the above expression, the Master Curve procedure was further simplified by making $K_{min} = 0$ such that the toughness distribution of K_{Jc}-values also follows a two-parameter Weibull distribution, similarly to the arguments presented in Section 4.2, thereby making contact with the two-parameter distribution of σ_w defined by Eq. (4). Moreover, such simplification is justified as T_0 exhibits only minor sensitivity to K_{min} in the range between 0 and 20 MPa$\sqrt{\text{m}}$ (which is the value adopted in ASTM E1921 [35]).

To explore the applicability of the procedure just outlined, this section describes estimation of the Weibull stress parameter, m, for the tested A572 Gr 50 steel using the approximate CVN energy correlation with the reference temperature, T_0. By adopting a hyperbolic tangent curve fitting of the CVN energy data shown in Fig. 3(b), B&R [40] report the Charpy transition temperatures corresponding to 28 J as $T_{CVN}^{28J} = -22°C \pm 15°C$ which then yields an estimate of $T_{0,\,med} = -40°C$ from Eq. (10) with bounds given by $T_{0,\,U} = -55°C$ and $T_{0,\,L} = -25°C$. Here, we note that the estimated value for the median reference temperature is lower than the T_0 temperature of −26°C evaluated by B&R [40] on the basis of the Master Curve methodology and the procedure given by ASTM E1921 [35]. On the other hand, further observe that $T_{0,\,L} = -25°C$ is very close to the T_0-value for this material - this aspect will be taken up in the discussion below.

With the T_0-values thus determined, an estimate of J_0 is found by substituting T_0 and the test temperature, $T = -20°C$ into Eq. (11) yielding $J_{0,\,med} = 95$ kJ/m^2, $J_{0,\,L} = 62$ kJ/m^2 and $J_{0,\,U} = 150$ kJ/ m^2. At this point, it becomes clear that the estimated median and upper bound values will provide nonconservative fracture predictions since $J_{0,\,med}$ and $J_{0,\,U}$ deviate rather significantly from the corresponding characteristic toughness describing the measure toughness distribution for the deeply-cracked specimen. However, limiting attention to the estimated lower bound value for J_0, the analysis can proceed to arrive at a lower bound prediction of fracture toughness. This choice can be justified based on the previous arguments in which $T_{0,\,L} = -25°C$ is very close to the reference temperature for the tested material evaluated by B&R [40]. Using now a weakest link scaling of $J_{0,\,L}$ to the corresponding value for, say, a 2T specimen configuration and performing the estimation procedure of parameter m with the finite element results already generated in previous section, the new estimated Weibull modulus becomes $m_L = 14$, which is the same as the previously estimated m-value for this material. Comparison of the fracture toughness prediction for the shallow crack specimen with $B = 12.5$ mm based on the estimated m_L-value with experimental data further illustrates the effectiveness of the approach. Fig. 9 displays the predicted fracture toughness distribution for this specimen configuration in which the dashed line defines the predicted lower bound values of fracture probability corresponding to a predicted J_0-value of 155 kJ/m^2 - see also Table 2. For reference, the predicted toughness distribution obtained previously and shown in Fig. 2(b) is also included in the plot and represented by the solid line.

While this exploratory application based on a rather simple procedure provides a slightly nonconservative fracture toughness prediction, the trends of the results displayed in Fig. 9 are encouraging, particularly when one considers the large constraint loss experienced by the shallow crack bend specimen under analysis associated with its reduced thickness and, more importantly, the very limited experimental data. In this regard, it is well to keep in mind that the analysis given here provides essentially a simplified route to conduct structural integrity assessments of cracked components without relying on cleavage fracture toughness testing. Consequently, one of the potential drawbacks in applying this approach is that reliable correlations of fracture toughness with CVN energy are required. Thus, since the present analysis is approximate in many respects, it will be difficult to draw definitive conclusions on the robustness of the procedure in the several cases that may arise in related applications, including fracture assessments of different classes of structural steels with varying hardening behavior and strength properties. The fuller verification of the procedure to address those cases is beyond the scope of the present work and a follow-up paper is planned on it.

7. Summary and conclusions

This work describes an alternative, simplified approach to estimate the Weibull stress parameter, m, using cleavage fracture toughness values measured from testing high constraint, standard fracture specimens. The estimation procedure builds upon the conventional toughness scaling model (TSM) based on the Weibull stress concept to correct measured toughness distributions for high constraint fracture specimens with identical in-plane dimensions but varying thickness. A central feature of the estimation strategy is that only one set of toughness data measured from standard specimens is needed to generate the statistical distribution of measured toughness values for use in the estimation method. The second toughness parameter required in the toughness scaling methodology derives from the application of the weakest link model (WLM) to describe the effects of thickness on cleavage fracture toughness. The approach thus requires a correspondence between predictions based upon the Weibull stress methodology and the weakest link model for measured toughness values under high constraint conditions.

Applications of the proposed procedure to analyze specimen geometry effects on fracture toughness values in a typical structural steel provide predictions that agree remarkably well with experimental data for shallow crack bend specimens with different thickness. In particular, the inherent difficulty in predicting the distribution of experimental fracture toughness for a shallow crack bend specimen with reduced thickness is greatly reduced. This specimen exhibits significant constraint loss with increased deformation as clearly indicated by the large fracture toughness elevation by approximately a factor of ≈ 3 with respect to the deeply-cracked 1T bend specimen. Given the very pronounced effect of a/W-ratio coupled with specimen thickness on J_c-values, these exploratory studies demonstrate the potential capability of the present approach to effectively correlate cleavage fracture behavior across different crack configurations thereby greatly simplifying engineering fracture assessments based upon the Weibull stress using limited laboratory fracture testing data. Additional analyses incorporating a further simplified approach based on the Master Curve methodology to estimate representative lower bound values of fracture toughness from CVN energy also provide predictions that agree relatively well with experimental data. While it is potentially less accurate than approaches relying on experimentally measured fracture toughness and, thus, appears to depend rather sensitively on the correlation of fracture toughness with CVN energy, it can advantageously be applied as a screening criterion in engineering fitness-for-service procedures for cracked components, provided more accurate and meaningful correlations of fracture toughness with CVN energy over a broad range of material properties become available. Indeed, the present simplified procedure to estimate parameter, m, shows promise in routine applications to assess the severity or significance of a crack-like flaw in engineering critical components, such as API 579 [12] or BS 7910 [13], as they could benefit from a relatively simpler σ_w-based fracture assessment methodology.

While we have not explored a broader range of crack configurations and loading modes, the operational simplicity and relatively modest effort required by the proposed estimation procedure, cast in the form of a toughness scaling approach coupled with the weakest link model, can greatly simplify engineering fracture assessments based upon the Weibull stress using limited fracture testing and, thus, encourages further investigations to improve on the present approach. Undoubtedly, a key feature in the success of the present methodology lies in assessing to what extent the often large variability in experimentally measured toughness values, coupled with accurate descriptions of the tensile response for the tested material, affect the estimated Weibull modulus

and, consequently, the predictive response of the Weibull stress approach. However, in view of the large simplification involved in the parameter estimation of the Weibull stress model, the potential sensitivity of the methodology to these issues does not seem to be unacceptable, providing conservative assessments are assured. Work along these lines is in progress.

CRediT author contribution statement

Vitor S. Barbosa: Formal analysis, Experimental Testing, Experimental data analysis, Writing - first draft. **C. Ruggieri**: Methodology development, Numerical analysis, Software development, Writing – final manuscript, review & editing, Supervision.

Declaration of competing interest

The authors declare that they have no known competing financial interests or personal relationships that could have appeared to influence the work reported in this paper.

Acknowledgments

This investigation is supported by Fundação de Amparo à Pesquisa do Estado de São Paulo (FAPESP) through research grant 2016/26024-1. The work of CR is also supported by the Brazilian Council for Scientific and Technological Development (CNPq) through grant 302853/2018-9. The authors acknowledge the many useful discussions and contributions of their colleague Prof. Robert H. Dodds (University of Illinois at Urbana-Champaign).

Appendix. Appendix - Measured J_c-Values for Shallow Crack SE(B) Specimens with $B = 12.5$ mm

We present here the results of additional fracture toughness tests performed on conventional, plane-sided three-point bend fracture specimens the T-L orientation for the ASTM A572 Gr 50 steel at $T = -20$°C described in Section 4.2. The tested geometry has $a/W = 0.2$, $W = 50$ mm, $S = 4W$ but a reduced thickness of 0.5T with $B = 12.5$ mm. The fracture mechanics test protocol followed rigorously the same procedures already reported by B&R [40]. Moreover, similarly to the previous experimental investigation of B&R [40], post-mortem examination of the fracture surfaces for all tested specimens revealed essentially no ductile tearing prior to cleavage fracture and clear characteristic of stress-controlled cleavage fracture. Table A.1 shows the fracture toughness at cleavage instability obtained from shallow crack SE(B) specimens with $a/W = 0.2$ and $B = 12.5$ mm tested at $T = -20$°C. The table also includes the average precrack fatigue length based on the 9-point measurement technique given by ASTM E1820 [47].

Table A.1
Measured cleavage fracture toughness values, described in terms of J_c, for the A572 Gr 50 steel obtained from shallow crack SE(B) specimens with $a/W = 0.2$ and $B = 12.5$ mm tested at $T = -20$°C.

Specimen Number	J_c [kJ/m^2]	a_0 [mm]	M=($b_0\sigma_{ys}/J_c$)
1	299	9.5	56
2	36	9.6	472
3	109	9.3	155
4	124	9.3	136
5	108	9.6	155
6	134	9.6	125
7	40	9.4	419
8	38	9.5	447
9	172	9.2	98
10	132	9.3	128
11	127	9.4	133
12	77	9.2	219
13	234	9.8	71
14	109	9.4	154
15	131	9.7	128

References

[1] R.H. Dodds, C. Shih, T. Anderson, Continuum and micro-mechanics treatment of constraint in fracture, Int. J. Fract. 64 (1993) 101–133.
[2] F.M. Beremin, A local criterion for cleavage fracture of a nuclear pressure vessel steel, Metall. Mater. Trans. 14 (1983) 2277–2287.
[3] C. Ruggieri, R.H. Dodds, An engineering methodology for constraint corrections of elastic-plastic fracture toughness - Part I: a review on probabilistic models and exploration of plastic strain effects, Eng. Fract. Mech. 134 (2015) 368–390.
[4] C. Ruggieri, R.H. Dodds, A local approach to cleavage fracture modeling: an overview of progress and challenges for engineering applications, Eng. Fract. Mech. 187 (2018) 381–403.
[5] C. Ruggieri, R.G. Savioli, R.H. Dodds, An engineering methodology for constraint corrections of elastic-plastic fracture toughness - Part II:: effects of specimen geometry and plastic strain on cleavage fracture predictions, Eng. Fract. Mech. 146 (2015) 185–209.
[6] A. Pineau, Development of the local approach to fracture over the past 25 years: theory and applications, Int. J. Fract. 138 (2006) 139–166.
[7] F. Minami, A. Brückner-Foit, D. Munz, B. Trolldenier, Estimation procedure for the Weibull parameters used in the local approach, Int. J. Fract. 54 (1992) 197–210.
[8] C. Ruggieri, R.H. Dodds, A transferability model for brittle fracture including constraint and ductile tearing effects: a probabilistic approach, Int. J. Fract. 79 (1996) 309–340.
[9] N.R. Mann, R.E. Schafer, N.D. Singpurwalla, Methods for Statistical Analysis of Reliability and Life Data, Jonh Wiley & Sons, New York, 1974.
[10] X. Gao, C. Ruggieri, R.H. Dodds, Calibration of Weibull stress parameters using fracture toughness data, Int. J. Fract. 92 (1998) 175–200.
[11] C. Ruggieri, X. Gao, R.H. Dodds, Transferability of elastic-plastic fracture toughness using the Weibull stress approach: significance of parameter calibration, Eng. Fract. Mech. 67 (2000) 101–117.
[12] American Petroleum Institute, Fitness-for-service, 2016. API RP-579-1/ASME FFS-1.
[13] British Institution, Guide to Methods for Assessing the Acceptability of Flaws in Metallic Structures, 2013. BS 7910.
[14] F. Mudry, A local approach to cleavage fracture, Nucl. Eng. Des. 105 (1987) 65–76.
[15] G.T. Hahn, The influence of microstructure on brittle fracture toughness, Metallurgical Transactions A 15 (1984) 947–959.
[16] A.A. Griffith, The phenomenon of rupture and flow in solids, Philosophical Transactions of the Royal Society, Series A 221 (1921) 163–198.
[17] W. Feller, Introduction to Probability Theory and its Application, vol. I, John Wiley & Sons, New York, 1957.
[18] A.G. Evans, T.G. Langdon, Structural ceramics, in: B. Chalmers (Ed.), Progress in Materials Science vol. 21, Pergamon Press, New York, 1976, pp. 171–441.
[19] T. Lin, A.G. Evans, R.O. Ritchie, A statistical model of brittle fracture by transgranular cleavage, J. Mech. Phys. Solid. 21 (1986) 263–277.
[20] X. Gao, R.H. Dodds, R.L. Tregoning, J.A. Joyce, L.R. Link, A Weibull stress model to predict cleavage fracture in plates containing surface cracks, Fatig. Fract. Eng. Mater. Struct. 22 (1999) 481–493.

[21] X. Gao, R.H. Dodds, Constraint effects on the ductile-to-brittle transition temperature of ferritic steels: a Weibull stress model, Int. J. Fract. 102 (2000) 43–69.
[22] X. Gao, R.H. Dodds, An engineering approach to assess constraint effects on cleavage fracture toughness, Eng. Fract. Mech. 68 (2001) 263–283.
[23] J.R. Petti, R.H. Dodds, Coupling of the Weibull stress model and macroscale models to predict cleavage fracture, Eng. Fract. Mech. 71 (2004) 2079–2103.
[24] J.R. Petti, R.H. Dodds, Calibration of the Weibull stress scale parameter, σ_u, using the master curve, Eng. Fract. Mech. 72 (2005) 91–120.
[25] C. Ruggieri, Influence of threshold parameters on cleavage fracture predictions using the Weibull stress model, Int. J. Fract. 110 (2001) 281–304.
[26] C. Ruggieri, An engineering methodology to assess effects of weld strength mismatch on cleavage fracture toughness using the Weibull stress approach, Int. J. Fract. 164 (2010) 231–252.
[27] A. Andrieu, A. Pineau, J. Besson, D. Ryckelynck, O. Bouaziz, Beremin model: methodology and application to the prediction of the euro toughness test, Eng. Fract. Mech. 95 (2012) 102–117.
[28] Y. Cao, H. Hui, G. Wang, F.Z. Xuan, Inferring the temperature dependence of beremin cleavage model parameters from the Master Curve, Nucl. Eng. Des. 241 (2011) 39–45.
[29] G. Qian, V.F. González-Albuixech, M. Niffenegger, Calibration of the beremin model with the master curve, Eng. Fract. Mech. 136 (2015) 15–25.
[30] J.W. Hutchinson, Singular behavior at the end of a tensile crack in a hardening material, J. Mech. Phys. Solid. 16 (1968) 13–31.
[31] J.R. Rice, G.F. Rosengren, Plane strain deformation near a crack tip in a power-law hardening material, J. Mech. Phys. Solid. 16 (1968) 1–12.
[32] J.W. Hutchinson, Fundamentals of the phenomenological theory of nonlinear fracture mechanics, J. Appl. Mech. 50 (1983) 1042–1051.
[33] E.J. Gumbel, Statistics of Extremes, Columbia University Press, New York, 1958.
[34] B. Epstein, Elements of the theory of extreme values, Technometrics 2 (1960) 27–41.
[35] American Society for Testing and Materials, Standard Test Method for Determination of Reference Temperature, T_0, for Ferritic Steels in the Transition Range, 2019. ASTM E1921-19.
[36] T.L. Anderson, Fracture Mechanics: Fundaments and Applications, third ed., CRC Press, Boca Raton, FL, 2005.
[37] M. Nevalainen, R.H. Dodds, Numerical investigation of 3-D constraint effects on brittle fracture in SE(B) and C(T) specimens, Int. J. Fract. 74 (1995) 131–161.
[38] C. Ruggieri, A probabilistic model including constraint and plastic strain effects for fracture toughness predictions in a pressure vessel steel, Int. J. Pres. Ves. Pip. 148 (2016) 9–25.
[39] R.G. Savioli, C. Ruggieri, Experimental study on the cleavage fracture behavior of an ASTM A285 Grade C pressure vessel steel, ASME Journal of Pressure Vessel Technology 137 (2) (2014) 1–7.
[40] V.S. Barbosa, C. Ruggieri, Fracture toughness testing using non-standard bend specimens - Part II: experiments and evaluation of t_0 reference temperature for a low alloy structural steel, Eng. Fract. Mech. 195 (2018) 297–312.
[41] B. Healy, A. Gullerud, K. Koppenhoefer, A. Roy, S. RoyChowdhury, J. Petti, M. Walters, B. Bichon, K. Cochran, A. Carlyle, J. Sobotka, M. Messner, R.H. Dodds, WARP3D: 3-D Nonlinear Finite Element Analysis of Solids for Fracture and Fatigue Processes, Tech. rep., University of Illinois at Urbana-Champaign, 2014. http://code.google.com/p/warp3d.
[42] B. Moran, C.F. Shih, A general treatment of crack tip contour integrals, Int. J. Fract. 35 (1987) 295–310.
[43] C. Ruggieri, WSTRESS Release 5.0: Numerical Evaluation of Probabilistic Fracture Parameters for 3-D Cracked Solids and Calibration of Weibull Stress Parameters, University of São Paulo, 2019. Tech. rep.
[44] C. Ruggieri, Dodds, Probabilistic modeling of brittle fracture including 3-d effects on constraint loss and ductile tearing, J. Phys. 6 (1996) 353–362.
[45] D.E. McCabe, J.G. Merkle, K. Wallin, An Introduction to the Development and Use of the Master Curve Method, ASTM International, 2005. ASTM Manual Series MNL 27.
[46] R.J. Smith, A.J. Horn, A.H. Sherry, Relating Charpy energy to fracture toughness in the lower transition region usin a Weibull stress dependent energy scaling model, Int. J. Pres. Ves. Pip. 166 (2018) 72–83.
[47] American Society for Testing and Materials, Standard Test Method for Measurement of Fracture Toughness, 2017. ASTM E1820-17.